0026-895X/86/050427-10$02.00/0

MOLECULAR PHARMACOLOGY, 30:427-436

Nicotinic Binding Sites in Rat and Mouse Brain: Comparison of Acetylcholine, Nicotine, and α-Bungarotoxin

MICHAEL J. MARKS, JERRY A. STITZEL, ELENA ROMM, JEANNE M. WEHNER, and ALLAN C. COLLINS
Institute for Behavioral Genetics and School of Pharmacy, University of Colorado, Boulder, Colorado 80309
Received May 12, 1986; Accepted July 28, 1986

SUMMARY

The properties of the binding sites for radiolabeled acetylcholine (measured in the presence of atropine), nicotine, and α-bungarotoxin were compared in brain tissue prepared from both rat and mouse. These three binding sites were tested for the following properties: affinity and density of ligand binding, effects of competitive inhibitors, regional distribution, effects of treatment with dithiothreitol and the reversal of these effects by treatment with 5,5′-dithiobis(2-nitrobenzoic acid), thermal lability, effects of protease treatment, and response to chronic administration of nicotine *in vivo*. The binding sites for acetylcholine and nicotine were affected identically for all measurements, whereas the binding site for α-bungarotoxin was affected in a manner different from that for the other two ligands. Although the regional distribution of nicotine and acetylcholine binding differed between rat and mouse brain, other properties of this binding site were very similar between the two species. The results are consistent with the proposal that acetylcholine and nicotine bind to the same sites in both rat and mouse brain, whereas α-bungarotoxin binds to different sites.

Several potential nicotinic receptor sites in brain have been identified by the binding of radiolabeled ligands. The snake neurotoxin, α-BTX, is one such ligand. This toxin binds to sites in the brain that have kinetic properties consistent with those anticipated for a nicotinic cholinergic receptor (1–3). In addition, the subunit composition of the α-BTX binding component isolated from chick brain closely resembles that of the nicotinic cholinergic receptor of muscle (4). However, snake α-toxins often fail to block nicotinic responses *in vivo* (5–7), leading to the suggestion that the toxin-binding sites are not really cholinergic receptors, or that additional nicotinic binding sites also exist in brain.

Based on the assumption that some nicotinic sites in the brain are cholinergic, the binding of [^{3}H]ACh (determined in the presence of atropine to inhibit binding to muscarinic sites) has been used to investigate potential receptor sites in rat brain (8). ACh binds saturably and reversibly. Classical nicotinic agonists are potent inhibitors of ACh binding, but most antagonists, including α-BTX, are less potent.

Radiolabeled nicotine, itself, has also been used to measure nicotinic sites in mammalian brain (9–13). Nicotine binds saturably and reversibly to brain tissue. Nicotine binding is inhibited by cholinergic agonists, but most cholinergic antagonists, including α-BTX, are poor inhibitors. The relative ineffectiveness of cholinergic antagonists to inhibit nicotine binding has led to the postulate that the nicotine-binding site is noncholinergic (9, 11, 14).

Comparison of the distribution of nicotine-binding sites in mouse brain regions or ACh-binding sites in rat brain regions to the distribution of the binding sites for α-BTX suggests that the sites labeled with α-BTX differed from those labeled with either nicotine or ACh (8, 12). An autoradiographic analysis of the distribution of the binding of these three ligands in rat brain has also demonstrated the difference between α-BTX binding and that of the other two ligands. In addition, the autoradiographic patterns observed for nicotine and ACh were strikingly similar, suggesting that these two ligands label the same binding sites (15). The binding of nicotine and ACh in brains of rodents treated chronically with nicotine changes in a similar, but unusual, pattern: nicotine binding in mice and ACh binding in rats increase with nicotine treatment (16–20). This unusual response to treatment with a classical nicotinic agonist in two different species further suggests that nicotine and ACh may be labeling the same sites in the brain.

Several inconsistencies in the properties of the binding sites for these two ligands have been observed. The regional distribution of nicotine binding in mouse brain does not correspond to that for ACh binding in rat brain (8, 12). This may be a species difference or a fundamental difference in the sites. When the regional distribution of nicotine and ACh binding

This work was supported by Grant DA-03194 from the National Institute on Drug Abuse and Grant AA-06391 from the National Institute on Alcohol Abuse and Alcoholism.

ABBREVIATIONS: α-BTX, α-bungarotoxin; ACh, acetylcholine; DFP, diisopropylfluorophosphate; DTNB, 5,5′-dithiobis-(2-nitrobenzoic acid); DTT, dithiothreitol; EDTA, ethylenediaminetetraacetic acid; HEPES, 4-(hydroxyethyl)-1-piperazineethanesulfonic acid.

were directly compared in two mouse strains, the patterns were not identical (21), but the fact that in some preparations nicotine displays two binding sites of different affinity, whereas ACh does not, confounds the regional comparisons. A nicotine-binding site has been purified from rat brain by affinity chromatography (22). In contrast to the four subunits observed for most nicotinic receptors, this material consisted of single protein component. This result suggests that the nicotine binding site is not a classical nicotinic cholinergic receptor, and that it may not be cholinergic at all.

The present study was undertaken to systematically compare the properties of the nicotine-, ACh-, and α-BTX-binding sites in both rats and mice to determine whether several properties of these binding sites were consistent with the proposal that nicotine and ACh label the same binding sites. The two species most widely used for investigations of nicotine effects were both examined. The results presented in this paper are consistent with the proposal that nicotine and ACh label the same population of binding sites, and that α-BTX clearly labels a distinct population of sites.

Materials and Methods

Animals. Mice of the strain DBA/2J/Ibg have been maintained in the colony at the Institute for Behavioral Genetics for more than 25 generations. Mice of either sex were housed with two to five like-sexed and like-aged animals. Mice were between 50 and 90 days of age when used.

Female Sprague-Dawley rats were purchased from Sasco Co., Omaha, NE. The rats were housed five per cage and weighed between 250 and 350 g when used.

Animals of the two species were housed in separate rooms. A 12-hr light/12-hr dark cycle (lights on 7 a.m. to 7 p.m.) was used. Animals were allowed free access to food (Wayne Lab Blox) and water.

Materials. The radiochemicals used in this study were obtained from the following sources: L-[^{3}H]nicotine (*N*-methyl-[^{3}H], specific activity 75.7 Ci/mmol) and α-[^{125}I]BTX (Tyr-[^{125}I], initial specific activity 132.6 Ci/mmol) were obtained from New England Nuclear, Boston, MA; [^{3}H]choline (*N*-methyl-[^{3}H], specific activity 80 Ci/mmol) was obtained either from New England Nuclear or Amersham Corp., Arlington Heights, IL.

Drugs and biochemicals were obtained from the following sources: L-nicotine, L-lobeline, hexamethonium bromide, decamethonium bromide, gallamine triethiodide, *d*-tubocurarine chloride, atropine sulfate, ACh iodide, carbamylcholine iodide, tetramethylammonium iodide, tetraethylammonium chloride, DFP, acetic anhydride, triethylamine, polyethyleneimine, Tris, Tris-HCl, DTNB, EDTA, protease from *Streptomyces griseus* (Pronase E), bovine serum albumin, α-BTX, and α-cobratoxin from Sigma Chemical Co., St. Louis, MO; HEPES and DTT from Boehringer-Mannheim, Indianapolis, IN; dimethylphenylpiperazinium chloride from Aldrich Chemical Co., Milwaukee, WI.; piperidine, DL-anabasine, and cytisine from Carl Roth through Atomergic Chemetals, Plainview, NY; D-nicotine as a generous gift from Dr. Takuro Kisaki of the Nippon Salt and Tobacco Institute.

Polypropylene test tubes were purchased from Sarstedt Co., Princeton, NJ. Glass fiber filters were obtained from Boehringer-Mannheim. Scintillation fluid (Safety Solve) was purchased from Research Products International, Mt. Prospect, IL.

Tissue preparation. Mice were killed by cervical dislocation and rats by decapitation. Each brain was removed and placed on an ice-cold platform. For most experiments, whole brain minus cerebellum was used. In the experiments in which the regional distribution of the binding sites was examined, the brains were dissected into eight regions: cerebral cortex, hindbrain (pons-medulla), cerebellum, hypothalamus, striatum, hippocampus, superior and inferior colliculi, and midbrain (primarily thalamus). Only six regions of chronically treated animals were dissected; cerebellum was discarded and the colliculi were included with midbrain.

After dissection, the brain or brain region was placed in 10 volumes of ice-cold buffer (Krebs-Ringer's HEPES: NaCl, 118 mM; KCl, 4.8 mM; $MgSO_4$, 1.2 mM; $CaCl_2$, 2.5 mM; HEPES, 20 mM, pH adjusted to 7.5 with NaOH). The tissue was homogenized using a Teflon pestle. The tissue preparation used was essentially that described by Romano and Goldstein (10). The homogenate was centrifuged at 18,000 × *g* for 20 min and the pellet was resuspended in 20 volumes of distilled water. After a 60-min incubation at 4°, the pellet was collected by centrifugation at 18,000 × *g* for 20 min. This pellet was subsequently resuspended in 10 volumes of Krebs-Ringer's HEPES and the suspension was centrifuged at 18,000 × *g* for 20 min. The buffer was discarded and 10 volumes of fresh Krebs-Ringer's HEPES were added. The sample was then frozen at −70° until assay. Prior to each centrifugation, the sample was incubated at 37° for 10 min to promote hydrolysis of endogenous ACh.

On the day of assay, the pellet was resuspended in the overlying buffer and DFP was added to a final concentration of 100 μM. The sample was then incubated at 37° for 10 min after which it was centrifuged at 18,000 × *g* for 20 min. The resulting pellet was then resuspended in Krebs-Ringer's HEPES containing 100 μM DFP for use in the assays.

L-[^{3}H]Nicotine binding. The binding of L-[^{3}H]nicotine was determined using a modification of the method of Romano and Goldstein (10) as described previously (12, 17, 20). In these experiments L-[^{3}H]nicotine binding was measured both at 4° and at 37° such that direct comparisons of the results obtained with these assays could be made to those for [^{3}H]ACh binding, which was performed at 4°, and for α-[^{125}I]BTX binding, which was performed at 37°.

Incubations were conducted in 12 × 75 mm polypropylene test tubes. Final incubation volume was 250 μl. The buffer used in these incubations was Krebs-Ringer's HEPES and 200 mM Tris buffer (pH 7.5 at the appropriate temperature) was also included in the incubations. The incubation time for binding at 4° was 2 hr (equilibrium reached at 1 hr) and at 37° was 5 min (equilibrium reached at 2 min). Samples contained 100–500 μg of protein. At the completion of the incubation period, samples were filtered in the cold room using apparatus which had been cooled to 4°. The binding reaction was terminated by diluting the samples with 3 ml of ice-cold buffer and followed immediately by filtration of the samples onto Boehringer-Mannheim glass fiber filters which had been soaked overnight in buffer containing 0.5% polyethyleneimine. Vacuum pressure was −50 to −100 torr. Samples routinely contained approximately 5 nM L-[^{3}H]nicotine. Blanks were established by including 10 μM nicotine in the samples.

The measurement of K_D and B_{max} were accomplished both by increasing the amount of radiolabeled compound in the incubation (to a concentration of 10 nM) and by adding nonlabeled nicotine to the incubations for concentrations greater than 10 nM. The binding constants were determined by linear regression analysis of Scatchard plots of the data.

The L-[^{3}H]nicotine was repurified by thin layer chromatography before use. The chromatogram was developed using Silica Gel G and a solvent system composed of $CHCl_3$:CH_3OH:NH_4OH (60:40:0.1). The nicotine was extracted with ethanol and stored frozen at −70° in ethanol/water containing a 5-fold molar excess of mercaptoacetic acid.

[^{3}H]ACh binding. [^{3}H]ACh was synthesized by reaction of [^{3}H]choline with acetic anhydride as described by Schwartz et al (8). The purity of the radiolabeled choline was checked prior to synthesis.

The binding of [^{3}H]ACh was measured using a modification of the method of Schwartz *et al.* (8). Incubations were conducted at 4° in polypropylene test tubes. Final incubation volume was 250 μl. Krebs-Ringer's HEPES was the principal buffer, but 20 mM Tris buffer (pH 7.5 at 4°) was added, as well. All incubations contained 5 μM atropine to inhibit the binding of [^{3}H]ACh to muscarinic receptors. The incubation time was 1 hr (equilibrium reached in 30 min). Samples contained 100–500 μg of protein. The binding reaction was terminated by

addition of 3 ml of buffer and filtration onto Boehringer-Mannheim glass fiber filters which had been soaked in buffer containing 0.5% polyethyleneimine. The filters were subsequently washed four more times with 3 ml of buffer. Vacuum pressure was −300 to −400 torr. Filtrations were conducted in the cold room with apparatus which had been cooled to 4°. Incubations routinely contained approximately 10 nM [^{3}H]ACh. Blanks were established by including 10 μM L-nicotine in the incubations.

The binding constants, K_D and B_{max}, were measured by increasing the concentration of [^{3}H]ACh to 20 nM and for higher concentrations by adding nonradioactive ACh. Constants were calculated by linear regression analysis of Scatchard plots.

α-[^{125}I]-BTX binding. The binding of α-[^{125}I]BTX was measured at 37° essentially as described previously (12, 17, 20). The binding buffer was Krebs-Ringer's HEPES containing 0.01% bovine serum albumin. Binding reactions were conducted in polypropylene test tubes in an incubation volume of 500 μl. Samples contained 50–250 μg of protein. Incubations were conducted for 4 hr (equilibrium reached in 2.5 hr). The binding reaction was terminated by dilution of the sample with ice-cold wash buffer and by filtration onto Boehringer-Mannheim glass fiber filters which had been soaked in buffer containing 0.5% polyethyleneimine. Wash buffer contained 0.05% polyetheleneimine. The filters were washed four additional times with 3-ml aliquots of buffer. Samples routinely contained approximately 2 nM α-[^{125}I]BTX. Blanks were established by including 1 mM L-nicotine in the incubation.

The binding constants K_D and B_{max} were determined from experiments in which increasing amounts of α-[^{125}I]BTX were included in the incubations. Binding constants were estimated by linear regression analysis of Scatchard plots.

Scintillation counting. After filtration, the washed glass fiber filters were placed in 7-ml plastic scintillation vials and 2.5 ml of Safety Solve were added to each vial. The vials were capped and mechanically shaken. Samples were counted on a Beckman 1800 Liquid Scintillation Spectrometer. Efficiency of counting was 45% for both ^{3}H and ^{125}I.

Protein assay. Protein was measured using the method of Lowry *et al.* (23) with bovine serum albumin as the standard.

Effects of competitive inhibitors. The effects of potential competitive inhibitors on the binding of L-[^{3}H]nicotine, [^{3}H]ACh, and α[^{125}I]BTX were examined by including the potential inhibitor in the incubations. Five concentrations chosen to bracket the IC_{50} values were used for each potential inhibitor. Inhibitors were added to the incubations prior to the addition of the radiolabeled ligand. When the effects of α-BTX and α-cobratoxin were examined, the tissue was incubated with the toxins for 2 hr at 37° prior to addition of the labeled compounds. This preincubation was included to allow the toxins to interact with the tissue since binding of these compounds is slow at 37° and virtually nonexistent at 4°.

Thermal denaturation. The stability of the binding sites to heat denaturation was determined by incubating the tissue at one of the following temperatures: 60° (10–40 min), 65° (10–40 min), 70° (5–30 min), 75° (2–20 min), and 80° (0.5–8 min). Buffer was warmed to the appropriate temperature and the incubation was begun by adding a concentrated aliquot of homogenate such that the final protein concentration was approximately 3 mg/ml. Aliquots were removed at four times during the incubation. Sampling times varied with temperature as indicated above. After removal, the aliquot was cooled to 4°. Samples were assayed for the binding of L-[^{3}H]nicotine, [^{3}H]ACh, and α-[^{125}I]BTX using the assay methods described above.

Effects of DTT. Aliquots of tissue homogenate were incubated with DTT (0.01–10 mM) for 10 min at 37°. At the completion of the incubation the samples were centrifuged at 18,000 × *g* for 20 min. The pellet was resuspended in buffer, and centrifuged at 18,000 × *g* for 20 min. The pellet was resuspended in buffer containing 100 μM DFP for assay of the binding of the three ligands.

Effects of treatment with DTNB after treatment with DTT. Tissue was first incubated with 1 mM DTT for 10 min at 37°. After the incubation, the samples were centrifuged at 18,000 × *g* for 20 min, the pellets were resuspended in buffer, and the samples were again centrifuged at 18,000 × *g* for 20 min. The resulting pellets were resuspended in buffer and aliquots were added to buffer containing DTNB (0.001–1 mM). Samples were incubated for 10 min at 37° and then centrifuged at 18,000 × *g* for 20 min. The pellets were washed by resuspension in fresh buffer followed by centrifugation at 18,000 × *g* for 20 min. These final pellets were resuspended in buffer containing 100 μM DFP for assay of the binding of the three ligands.

Effects of Pronase E treatment. Homogenates which had not yet been treated with DFP were incubated at 37° with 1 mg/ml of Pronase E with constant shaking for 1 hr. At the conclusion of the incubation, DFP and EDTA were added to give final concentrations of 100 μM and 5 mM, respectively. The samples were then centrifuged at 18,000 × *g* for 20 min. The pellets were resuspended in buffer and these samples were centrifuged at 18,000 × *g* for 20 min. These final pellets were resuspended in buffer for assay of the binding of the three ligands. Pronase concentrations ranging from 0.2 to 20 mg/ml and incubation times between 5 and 120 min were also examined.

Chronic treatment with nicotine. Both rats and mice were chronically treated with nicotine to determine the effects of these treatments on the binding of the three ligands.

Rats were treated by subcutaneous injection of saline or 0.8 mg/kg or 1.6 mg/kg of nicotine base twice daily for 5 or 9 days. Injection solutions were neutralized with HCl. At the end of the treatment period, the rats were decapitated and the brains were dissected into six regions. Mice were treated by constant intravenous infusion of saline or 2.0, 4.0, or 6.0 mg/kg/hr of nicotine base. Solutions were neutralized with HCl. Chronic drug treatments were conducted as described in detail elsewhere (17, 20). Treatment at final dose was for 8–10 days. At the end of the treatment period, mice were killed by cervical dislocation and their brains were dissected into six regions.

Data analysis. Binding constants were calculated by linear regression of Scatchard plots. IC_{50} values were calculated from log dose response curves of inhibition experiments. Estimates of the K_I values were made using the equation of Cheng and Prusoff (23a). Correlations between the binding of any two ligands were determined by linear regression analysis. This analysis was applied to the following results: K_I values (on a log-log scale), regional distribution of binding sites, effect of DTT treatment, effects of DTNB reversal of DTT treatment, and regional distribution of binding sites after chronic drug treatment. One-way analysis of variance was used to test for the effects of chronic nicotine on the binding of each ligand in each region of rat and mouse brain. The first order decay curves for the thermal denaturation experiments were tested for parallelism and superimposability (i.e., identity of the lines) with *t* tests.

Results

The results that follow are a series of comparisons of the properties of binding sites measured with L-[^{3}H]nicotine, [^{3}H]ACh, and α-[^{125}I]BTX. Measurements were made using tissue prepared from both rat and mouse brain. In addition, L-[^{3}H]nicotine binding was measured at both 4° and 37° to provide direct comparison to the binding of [^{3}H]ACh and α-[^{125}I]BTX, respectively. The different incubation temperatures were necessitated because [^{3}H]ACh binding is poor at 37° and α-[^{125}I]BTX binding fails to reach equilibrium after 24 hr at 4°. The results of these direct comparisons should provide further evidence of the nature of the three nicotinic ligands and should provide additional tests to determine whether these ligands bind to different sites.

Saturability of binding sites. The results presented in Fig. 1 are Scatchard plots for the binding of L-[^{3}H]nicotine, [^{3}H]ACh, and α-[^{125}I]BTX to particulate fractions prepared from mouse and rat brain. The Scatchard plots for the binding

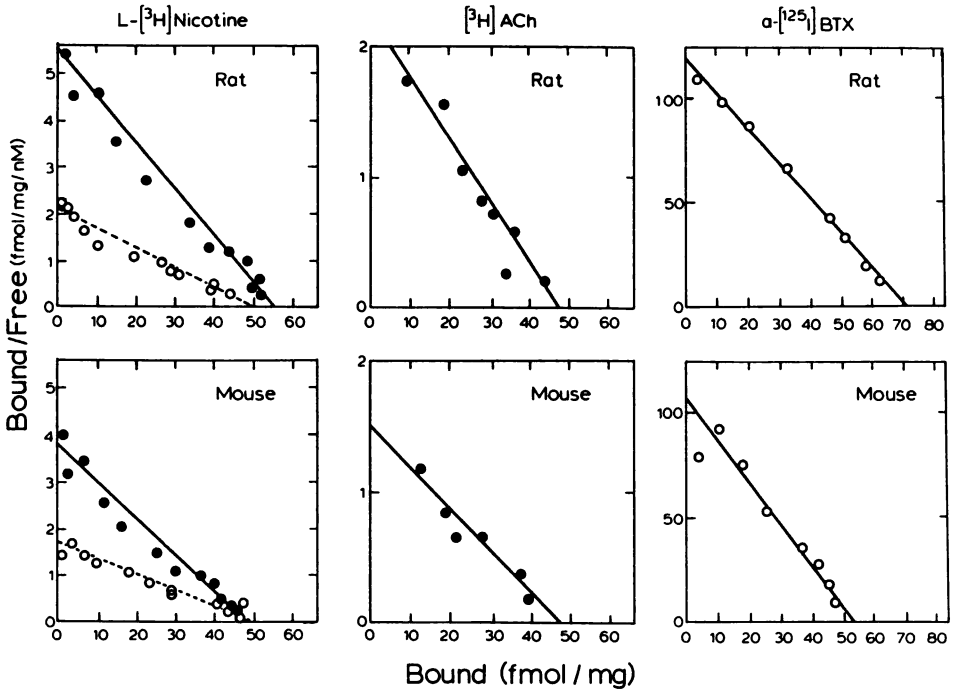

Fig. 1. Scatchard plots. Saturation curves for the binding of the three ligands were determined in rat and mouse brains. The binding of L-[^{3}H]nicotine was measured at both 4° (●) and 37° (○).

of all three ligands are linear. The K_D values for nicotine binding differed at the two incubation temperatures: the affinity of nicotine for its binding site at 4° was approximately twice the affinity at 37°. The incubation temperature had no effect on the B_{max} values. Although the B_{max} values in mouse brain tended to be slightly lower for all three ligands, the B_{max} for L-[^{3}H]nicotine binding did not differ from that for [^{3}H]ACh binding in either species. The B_{max} values for α-[^{125}I]BTX binding were approximately 20% higher than the B_{max} values for the other two ligands.

Competitive inhibition of ligand binding. The inhibition of L-[^{3}H]nicotine, [^{3}H]ACh, and α-[^{125}I]BTX binding by nicotinic agonists and antagonists was measured and the K_I values for these compounds are summarized in Table 1. The compounds tested displayed similar potency for inhibition of the ligands in rat and mouse tissue. In general, nicotinic agonists were more potent inhibitors of the binding of L-[^{3}H]nicotine and [^{3}H]ACh than were nicotinic antagonists. Whereas several agonists were considerably more potent inhibitors of L-[^{3}H]nicotine and [^{3}H]ACh binding than of α-[^{125}I]BTX (L-nicotine, D-nicotine, cytisine, lobeline, ACh, and carbamylcholine), several agonists were equally effective inhibitors of all three ligands (anabasine, dimethylphenylpiperazinium, piperidine, and tetramethylammonium). Although L-nicotine was 20–30-fold more potent than D-nicotine as an inhibitor of L-[^{3}H]nicotine and [^{3}H]ACh binding, it was only about 4-fold more potent as an inhibitor of α-[^{125}I]BTX binding.

With the exception of *d*-tubocurarine, which displayed a K_I for inhibition of α-[^{125}I]BTX that was 10-fold lower than that for the other two ligands, the classical antagonists were approximately equipotent for all three ligands.

The two snake α-toxins tested were potent inhibitors of α-[^{125}I]BTX binding but had no effect on either L-[^{3}H]nicotine binding or [^{3}H]ACh binding at concentrations as high as 100 nM.

The K_I values were subsequently examined graphically in order to provide a more direct comparison of the potency of the cholinergic agents in inhibiting the binding of the three ligands. The results displayed in Fig. 2 examine the relationship between the log of the K_I values obtained for L-[^{3}H]nicotine and [^{3}H]ACh and for L-[^{3}H]nicotine and α-[^{125}I]BTX in both rats and mice. Linear regression analyses of these data demonstrate that the K_I values obtained for L-[^{3}H]nicotine and [^{3}H]ACh are highly correlated for both rat ($r = 0.98$) and mouse ($r = 0.99$) brain tissue. The K_I values obtained for inhibition of L-[^{3}H]nicotine and for inhibition of α-[^{125}I]BTX are less closely correlated. If the values for α-BTX and α-cobratoxin are omitted, the correlation constants are modest for both rat ($r = 0.79$) and mouse ($r = 0.80$). However, if the values for the toxins are included, the correlation is completely lost (rat, $r = 0.14$; mouse, $r = 0.04$).

Since the K_D values for L-[^{3}H]nicotine and [^{3}H]ACh binding were determined under the same conditions as the K_I for the inhibition of L-[^{3}H]nicotine binding by ACh and of [^{3}H]ACh binding by L-nicotine, the K_D and K_I values can be directly compared. In the rat brain, the K_D for L-[^{3}H]nicotine binding was 13.8 ± 1.3 nM, whereas the K_I for L-nicotine inhibition of [^{3}H]ACh binding was 6.7 ± 1.5 nM. In the mouse brain, these values were 10.1 ± 0.4 and 7.3 ± 3.8 nM, respectively. In neither species did the K_D for L-nicotine binding differ from its K_I for inhibition of [^{3}H]ACh binding. In the rat brain, the K_D for [^{3}H]ACh binding was 37.4 ± 3.9 nM and the K_I for ACh inhibition of L-[^{3}H]nicotine binding was 44 ± 4 nM. In the mouse brain, these values were 37.1 ± 7.2 nM and 41 ± 28 nM, respectively. In neither species did the K_D for [^{3}H]ACh binding differ from the K_I for ACh inhibition of L-[^{3}H]nicotine binding.

Regional distribution of ligand binding. Both rat brain and mouse brain were dissected into eight regions, each of which was assayed for the binding of L-[^{3}H]nicotine, [^{3}H]ACh, and α-[^{125}I]BTX. The results presented in Fig. 3 compare the regional distribution for the binding of these three ligands in both species.

TABLE 1

Inhibition of L-[^{3}H]nicotine, [^{3}H]ACh, and α-[^{125}I]BTX binding

The K_i values (μM) were calculated from ED_{50} values from inhibition curves for each ligand. The binding of L-[^{3}H]nicotine was measured both at 4° and 37° as indicated. The ligand concentrations used in these experiments were: L-[^{3}H]nicotine, 4.5 ± 0.2 nM; [^{3}H]ACh, 11.1 ± 0.5 nM; and α-[^{125}I]BTX, 1.92 ± 0.10 nM. Values given are means for triplicate determinations, with standard errors in parentheses.

Inhibitor	Rats				Mice			
	ACh	Nicotine		α-BTX	ACh	Nicotine		α-BTX
		4°	37°			4°	37°	
1. Cytisine	0.0020 (0.0029)	0.0015 (0.0007)	0.0030 (0.0021)	1.4 (0.3)	0.0016 (0.0037)	0.0011 (0.0005)	0.0022 (0.0015)	1.1 (0.2)
2. L-Nicotine	0.0067 (0.0015)	0.0104 (0.0033)	0.0142 (0.0049)	0.82 (0.36)	0.0073 (0.0038)	0.0080 (0.0060)	0.015 (0.003)	0.62 (0.07)
3. D-Nicotine	0.36 (0.09)	0.33 (0.09)	0.28 (0.03)	3.0 (0.5)	0.33 (0.06)	0.24 (0.18)	0.23 (0.04)	2.8 (0.7)
4. Acetylcholine	0.051 (0.014)	0.044 (0.006)	0.120 (0.010)	4.0 (1.2)	0.052 (0.027)	0.041 (0.025)	0.088 (0.005)	3.1 (0.3)
5. Carbamylcholine	1.1 (0.3)	1.0 (0.2)	1.2 (0.2)	12.0 (2.0)	0.8 (0.5)	0.9 (0.2)	1.1 (0.1)	13.0 (4.0)
6. L-Lobeline	0.17 (0.25)	0.05 (0.02)	0.24 (0.10)	11.0 (4.0)	0.10 (0.05)	0.05 (0.02)	0.16 (0.01)	10.0 (3.0)
7. Dimethylphenyl-piperazinum	0.30 (0.14)	0.19 (0.05)	0.20 (0.03)	0.47 (0.06)	0.09 (0.15)	0.14 (0.10)	0.19 (0.04)	0.68 (0.28)
8. Anabasine	0.59 (0.13)	0.52 (0.11)	0.26 (0.12)	0.34 (0.05)	0.86 (0.07)	0.51 (0.13)	0.25 (0.03)	0.33 (0.45)
9. Tetramethyl-ammonium	4.4 (1.6)	2.8 (0.6)	2.2 (0.7)	1.8 (0.3)	5.4 (2.2)	2.9 (0.8)	1.8 (0.6)	2.2 (0.3)
10. Piperidine	120 (20)	28 (6)	22 (10)	23 (17)	9.8 (7.6)	40 (16)	13 (4)	21 (10)
11. *d*-Tubocurarine	59 (18)	81 (19)	33 (7)	2.8 (1.2)	96 (34)	100 (12)	40 (9)	3.7 (1.0)
12. Decamethonium	24 (9)	27 (6)	16 (6)	25 (6)	41 (4)	26 (3)	17 (4)	20 (5)
13. Gallamine	100 (30)	350 (190)	170 (50)	120 (30)	290 (250)	360 (70)	250 (50)	96 (37)
14. Hexamethonium	1000 (200)	760 (80)	720 (170)	540 (490)	1200 (800)	540 (400)	790 (60)	540 (470)
15. Tetraethyl-ammonium	2300 (3700)	350 (120)	80 (19)	42 (10)	570 (150)	550 (190)	86 (5)	25 (9)
16. α-Bungarotoxin	>100	>100	>100	0.00016 (0.00017)	>100	>100	>100	0.00013 (0.00005)
17. α-Cobratoxin	>100	>100	>100	0.0026 (0.0013)	>100	>100	>100	0.0021 (0.0011)

The patterns of L-[^{3}H]nicotine and [^{3}H]ACh binding were very similar in both species as demonstrated by the high correlation between these two parameters (r = 0.99 for rat and r = 0.98 for mouse). In contrast, the patterns of distribution for L-[^{3}H]nicotine and α-[^{125}I]BTX binding were dissimilar (r = −0.33 for rat and r = 0.36 for mouse).

Whereas the pattern of regional distribution of the binding sites for the three ligands were comparable between the two species, the absolute and relative binding of the ligands differed between rat and mouse. The binding of L-[^{3}H]nicotine and [^{3}H]ACh was higher in cortex, cerebellum, and striatum of the rat. In contrast, the binding of L-[^{3}H]nicotine and [^{3}H]ACh was higher in the midbrain, hypothalamus, and colliculi of the mouse. The binding of α-[^{125}I]BTX was higher in hindbrain, hippocampus, hypothalamus, and colliculi of the rat. Mouse striatum, however, displayed α-[^{125}I]BTX binding approximately 6-fold higher than that of rat striatum.

Effect of DTT. The effect of treatment with several concentrations of DTT on the binding of L-[^{3}H]nicotine, [^{3}H]ACh, and α-[^{125}I]BTX in rat and mouse are shown in Fig. 4. DTT treatment reduced the binding of all three ligands in a concentration-dependent manner. Binding of both L-[^{3}H]nicotine and [^{3}H]ACh was reduced to one-half of control binding by treatment with approximately 500 μM DTT in both species. Incubation temperature did not affect the pattern observed for the effects on L-[^{3}H]nicotine binding. A higher concentration of DTT was required to reduce α-[^{125}I]BTX binding to 50% of control, but the inhibition occurred over a wider range of concentrations. Correlations of the effects of DTT treatment on L-[^{3}H]nicotine binding and [^{3}H]ACh binding were high (r = 0.99 for rat and r = 0.97 for mouse), indicating that the effects of this reagent on the binding sites for the two ligands were very similar. Correlations of the effects of treatment on α-[^{125}I]BTX binding and L-[^{3}H]nicotine binding were also substantial (r = 0.87 for rat and r = 0.96 for mouse), suggesting that the effects of DDT on these two binding sites were also similar.

The reduction of the binding resulted from decreases in the apparent B_{max} for the binding. The K_D values were unaffected (data not shown).

Reversal of DTT effects by treatment with DTNB. The results shown in Fig. 5 demonstrate the effects of incubation with various concentrations of DTNB on the binding of the three ligands to tissue that had previously been treated with 1 mM DTT. The inhibition observed after treatment with this concentration of DTT was 80–90% for [^{3}H]ACh and L-[^{3}H]nicotine binding and 25–40% for α-[^{125}I]BTX binding. The effects of DTT are reversed by treatment with DTNB in a

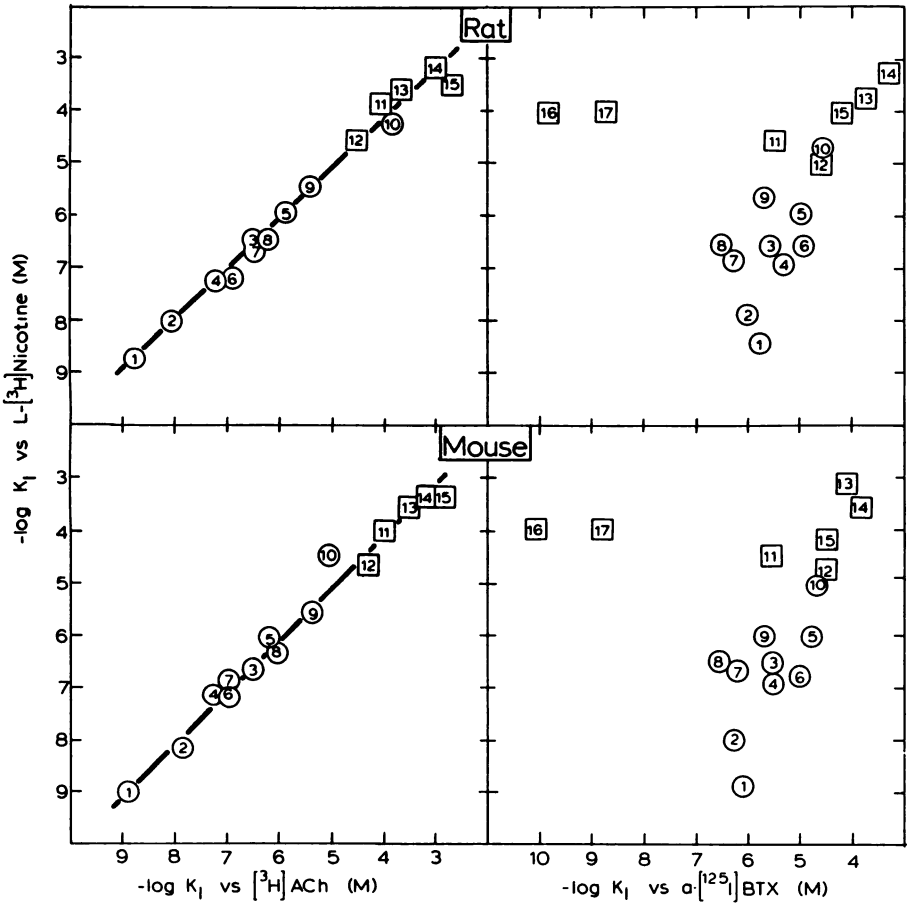

Fig. 2. Relationship of inhibitor potency. Log-log plots of K_I values determined for each of the ligands are plotted for comparison of the relative potency of the various inhibitors listed in Table 1. Mean ± standard error values for agonists (○) and antagonists (□) are shown. The equations of the various lines are: *Rat*, K_I for ACh versus K_I for nicotine, $Y = 0.96X - 0.39$, $r = 0.98$; *Rat*, K_I for α-BTX versus K_I for nicotine (omitting toxins), $Y = 1.36X + 0.73$, $r = 0.79$, and, including toxins, $Y = 0.15X - 4.73$, $r = 0.14$; *Mouse*, K_I for ACh versus K_I for nicotine – $Y = 1.04X + 0.24$, $r = 0.99$; *Mouse*, K_I for α-BTX versus K_I for nicotine (omitting toxins), $Y = 1.72X + 2.37$, $r = 0.80$, and, including toxins, $Y = 0.39X - 5.31$, $r = 0.04$. Assays were conducted at 4° for ACh and nicotine comparisons and at 37° for nicotine and α-BTX comparisons. For analysis of the effects of the toxins, tissue was incubated with the appropriate toxin for 2 hr before the binding assay was begun.

concentration-dependent fashion. Under these conditions the concentration of DTNB required for 50% reversal was 20–30 μM for all ligands in both species. The concentration dependence for reversal of DTT effects by DTNB treatment was similar for [^{3}H]ACh and L-[^{3}H]nicotine in rats ($r = 0.99$) and mice ($r = 0.96$). The pattern of reversal for α-[^{125}I]BTX binding and L-[^{3}H]nicotine binding was not as similar ($r = 0.96$ for rat, $r = 0.76$ for mouse). Treatment of the tissue with 1 mM DTNB had little effect on the binding of any ligand.

Thermal sensitivity of the binding sites. The results shown in Fig. 6 are the values for the slopes of the first order decay curves generated by heating tissue at 60°, 65°, 70°, 75°, or 80° for varying lengths of time. Increasing the temperature decreases the stability of the binding site for each ligand. The binding site for α-[^{125}I]BTX is more stable to thermal denaturation at 75° and 80° than are the binding sites for either [^{3}H]ACh or L-[^{3}H]nicotine. The sensitivity to thermal denaturation of the [^{3}H]ACh and L-[^{3}H]nicotine binding sites is the same at all five temperatures in both species: no differences in the decay constants were observed.

Heating had no significant effect on the K_D values; decreases in binding resulted from decreases in B_{max} (results not shown).

Effects of protease treatment. The effects of incubation of the tissue with protease isolated from *S. griseus* (Pronase E) are summarized in Table 2. Protease treatment (1 mg/ml for 1 hr at 37°) decreased the protein content in the particulate fraction by approximately 40%. The binding of α-[^{125}I]BTX was reduced by approximately 95% in both species. Both the total binding and the specific activity were affected by protease treatment. This effect did not result from the presence of protease in the tissue during the binding assay since mixing of protease-treated tissue with untreated tissue gave binding equivalent to the sum expected from each source. In contrast, the specific activity of neither [^{3}H]ACh binding nor L-[^{3}H]nicotine was reduced by more than 20% by protease treatment. The total number of binding sites was reduced by approximately 50%, a value slightly greater than that observed for the bulk particulate protein.

Response of the binding sites to chronic nicotine treatment. Chronic nicotine injection of rats resulted in an overall increase in both [^{3}H]ACh and L-[^{3}H]nicotine binding in cortex, hippocampus, and hypothalamus. The binding of these two ligands in the other three regions and of α-[^{125}I]BTX in all six regions was not significantly changed by the treatments. The relationship among the binding of the three ligands in the six brain regions of the three treatment groups is summarized in Fig. 7. Drug treatment had similar effects on the binding of [^{3}H]ACh and L-[^{3}H]nicotine as evidenced by the high correlation between the binding of these two ligands ($r = 0.95$). No significant relationship between α-[^{125}I]BTX and L-[^{3}H]nicotine binding was observed ($r = -0.33$).

The relationship among the binding of the three ligands in six regions of mice chronically infused with nicotine is also shown in Fig. 7. Owing to tissue limitations, one set of mice served as the source of tissue for the measurement of [^{3}H]ACh and L-[^{3}H]nicotine binding and another set as the source of tissue for measurement of α-[^{125}I]BTX and L-[^{3}H]nicotine binding. Chronic nicotine infusion resulted in a significant increase in both [^{3}H]ACh and L-[^{3}H]nicotine binding in all six regions and in a significant increase in α-[^{125}I]BTX binding in

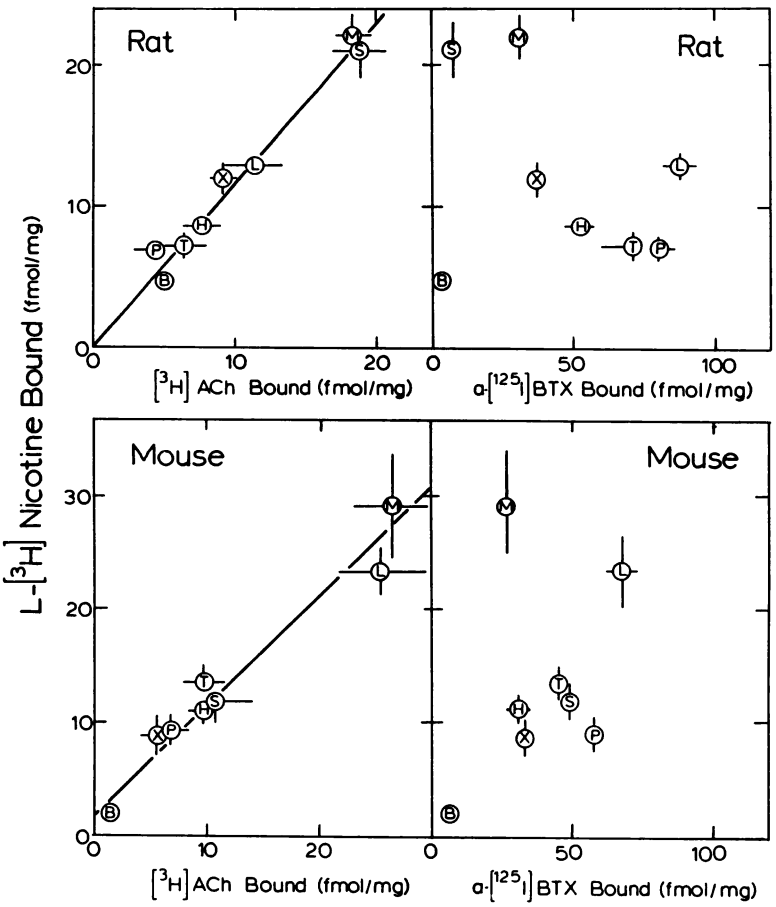

Fig. 3. Comparison of regional distribution of binding. Rat and mouse brains were dissected into eight regions as described in Materials and Methods, and the binding of the three ligands was measured in each region. Assays were conducted using a single concentration of each ligand: L-[^{3}H]nicotine, 4.8 ± 0.1 nM; [^{3}H]ACh, 9.9 ± 0.7 nM; and α-[^{125}I]BTX, 1.73 ± 0.06 nM. The figures show the amount of L-[^{3}H]nicotine binding measured in each region as a function of the binding of each of the other two ligands. The brain regions are identified by the following symbols: *X*, cortex, *B*, cerebellum; *H*, hindbrain; *P*, hippocampus; *S*, striatum, *T*, hypothalamus; *L*, colliculi; and *M*, midbrain. Each *point* represents the mean ± standard error of six measurements. The equations of the lines are: *rat*, ACh binding versus nicotine binding, $Y = 1.14X + 0.42$, $r = 0.99$; *Rat*, α-BTX binding versus nicotine binding, $Y = -0.06X + 15.12$, $r = -0.33$; *Mouse*, ACh binding versus nicotine binding, $Y = 0.93X + 2.39$, $r = 0.98$; and *Mouse*, α-BTX binding versus nicotine binding, $Y = 0.16X + 7.32$, $r = 0.36$.

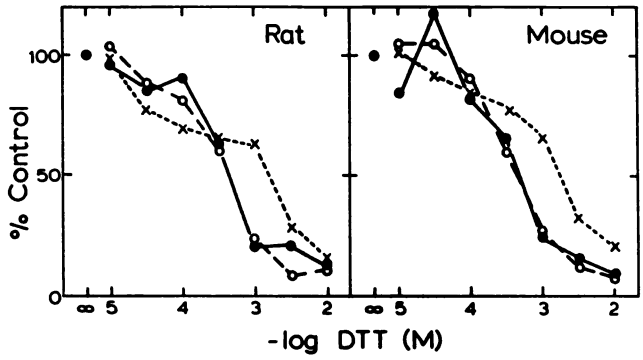

Fig. 4. Effect of DTT. Tissue was incubated with the indicated concentrations of DTT, washed, and incubated with a single concentration of one of the three ligands: L-[^{3}H]nicotine, 4.1 nM (●); [^{3}H]ACh, 13.0 nM (○), or α-[^{125}I]BTX, 1.81 nM (×). Each *point* is the mean obtained from two separate experiments. Control binding for the ligands was: L-[^{3}H:]nicotine, rat = 17.8 fmol/mg and mouse = 17.6 fmol/mg; [^{3}H]ACh, rat = 20.1 fmol/mg and mouse = 20.2 fmol/mg; and α-[^{125}I]BTX, rat = 51.8 fmol/mg and mouse = 46.8 fmol/mg.

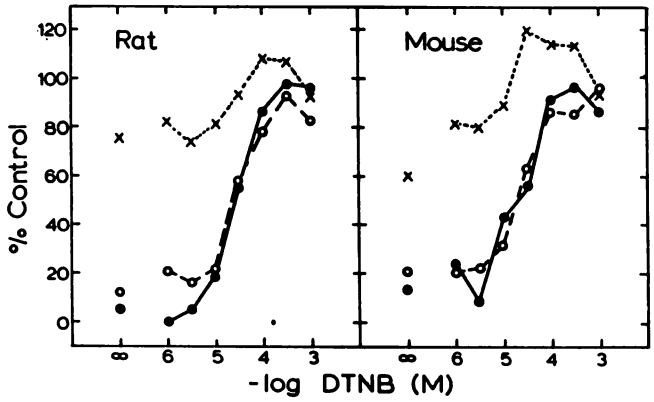

Fig. 5. Reversal of DTT effects with DTNB. Tissue was incubated with 1 mM DTT, washed, and then treated with the concentrations of DTNB indicated. After the DTNB treatment, the tissue was washed and the binding of the three ligands was measured. The concentrations of the ligands used were: L-[^{3}H]nicotine = 4.8 nM (●), [^{3}H]ACh = 11.8 nM (○), and α-[^{125}I]BTX = 1.87 nM (×). Each *point* represents the mean of two separate experiments. The control binding values of the various ligands were: L[^{3}H]nicotine, rat = 19.6 fmol/mg and mouse = 19.7 fmol/mg; [^{3}H]ACh, rat = 18.8 fmol/mg and mouse = 21/4 fmol/mg; and α-[^{125}I]BTX, rat = 44.4 fmol/mg and mouse = 35.7 fmol/mg.

cortex, hippocampus, hindbrain, and hypothalamus. Chronic nicotine infusion had similar effects on the binding of [^{3}H]ACh and L-[^{3}H]nicotine: the amount of binding measured with these two ligands is closely correlated ($r = 0.96$). The binding of α-[^{125}I]BTX and L-[^{3}H]nicotine binding are not closely correlated, however ($r = -0.18$).

Discussion

The properties of the binding sites for [^{3}H]ACh and L-[^{3}H]nicotine have been examined in parallel with the following results: the numbers of binding sites in whole brain are the same, the K_D for L-[^{3}H]nicotine binding corresponds to its K_I in inhibiting [^{3}H]ACh binding and the K_D for [^{3}H]ACh binding corresponds to its K_I for inhibiting L-[^{3}H]nicotine binding, the inhibitory potency of many nicotinic agents at both binding sites is virtually identical, the regional distributions of the

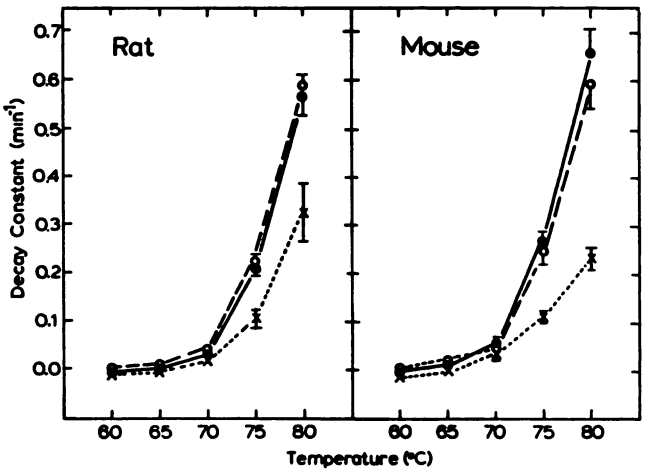

Fig. 6. Effect of elevated temperature. Tissue was incubated at one of the five temperatures indicated and aliquots were periodically removed and cooled. Tissue was subsequently assayed for the binding of the three ligands using the following concentrations: L-[^{3}H]nicotine = 4.7 nM (●); [^{3}H]ACh = 11.8 nM (○); and α-[^{125}I]BTX = 1.88 nM (×). The values shown represent the mean ± standard error for the slopes of the first order decay curves for each ligand at each temperature. The slopes for the α-BTX curves for both rat and mouse tissue differ from those for both nicotine and ACh at 75° and 80°.

binding sites correspond, the binding sites are identically affected by treatment with DTT, the DTT inhibition is identically reversed by treatment with DTNB, the sensitivity of the binding sites to thermal denaturation is the same, treatment with a protease has the same effect on both sites, and both binding sites respond in identical fashion to chronic nicotine treatment. The series of observations listed above is completely consistent with the hypothesis that [^{3}H]ACh and L-[^{3}H]nicotine bind to the same sites in both rat and mouse brain. Martino *et al.* (24) reached the same conclusion after direct comparison of the binding of these two ligands in rat brain. The observations are also consistent with the pattern of regional distribution of the binding of the two ligands as examined autoradiographically (15).

The binding site for α-[^{125}I]BTX is not the same as the ACh/nicotine site. The properties of the α-[^{125}I]BTX site differ from those of the ACh/nicotine site for nearly all of the criteria listed above. The contention that these two nicotinic sites differ is consistent with previous observations of the kinetic properties of these sites (8, 12) and of their autoradiographic distribution (15). The nicotine-binding site does appear to be unusual in that the potency of nicotinic antagonists is much lower than is the potency of the agonists. Inspection of the data contained in Table 1 reveals, however, that the potency of the antagonists is very similar at the ACh/nicotine site and at the α-BTX site.

The results presented in this paper suggest that the properties of the two classes of nicotinic binding sites are very similar in rat and mouse brain, inasmuch as the K_D values are similar, the K_I values for many inhibitors are comparable, and the sensitivities to treatment with DTT, protease, and heat are also comparable. Although the properties of the nicotinic sites are nearly identical, their distribution in the brains of the two species differs markedly. An autoradiographic analysis of nicotinic binding sites in mouse brain is required to provide a more detailed comparison to that obtained in rat brain. The regional distributions for ACh/nicotine binding in rat brain for two well defined regions (relative to cerebral cortex) can be compared to those obtained from a semiquantitative autoradiographic analysis of ACh binding (25) (relative hippocampal binding 0.64 by dissection, 0.61 by autoradiography; relative hypothalamic binding 0.55 by dissection, 0.57 by autoradiography). Although dissection can not achieve the level of resolution attained with autoradiography, it appears that, when direct comparisons can be made, the results obtained with the two methods are comparable. If the pharmacological effects of nicotine are regulated in part through α-BTX- and ACh/nicotine-binding sites, the difference in the regional distribution of these sites suggests that the central effects of nicotine may occur through different neuronal pathways in these two species.

The patterns of regional distribution of L-[^{3}H]nicotine binding and [^{3}H]ACh binding presented in this paper are identical in the two species tested. This result would appear to be in conflict with a previous report that regional distribution of the binding of these two ligands differed in two mouse strains (21). It should be noted that the previous study measured both high and low affinity nicotine binding, a fact which may have obscured the relationship between the high affinity binding of these two ligands.

The binding of L-[^{3}H]nicotine reported in this paper occurs

TABLE 2

Binding after Pronase treatment

Prior to treatment with DFP, tissue was incubated for 1 hr at 37° with 1 mg/ml of Pronase. After incubation, DFP and EDTA were added to final concentrations of 100 μM and 5 mM, respectively. The samples were washed by centrifugation and the tissue was assayed for protein and ligand binding. Control samples were incubated at 37° without Pronase. Values represent mean ± standard error for three separate experiments. Protein content is expressed as mg/ml, the specific activity of ligand binding is fmol/mg of protein, and the total ligand binding is expressed as fmol. Ligand concentrations used in the assays were: L-[^{3}H]nicotine, 4.4 ± 0.4 nM; [^{3}H]ACh, 13.6 ± 1.2 nM; and α-[^{125}I]BTX, 1.96 ± 0.1 nM.

Parameter	Before treatment		After treatment		
	specific activity	Total/ml	Specific activity	Total/ml	Percentage control
Rat					
Protein		3.03 ± 0.33		1.70 ± 0.26	56.4 ± 6.7
L-[^{3}H]Nicotine	23.4 ± 4.2	68.3 ± 4.2	20.0 ± 3.1	33.6 ± 5.6	50.7 ± 9.9
[^{3}H]ACh	16.2 ± 0.1	49.0 ± 5.5	12.7 ± 1.5	22.1 ± 5.9	45.6 ± 10.9
α-[^{125}I]BTX	48.9 ± 1.7	147.9 ± 18.3	6.4 ± 0.4	11.0 ± 4.8	6.9 ± 2.6
Mouse					
Protein		3.30 ± 0.17		1.98 ± 0.08	60.6 ± 4.8
L-[^{3}H]Nicotine	18.4 ± 0.5	60.4 ± 1.9	15.0 ± 1.2	29.9 ± 3.3	50.5 ± 6.9
[^{3}H]ACh	19.6 ± 1.4	65.0 ± 7.7	15.4 ± 1.0	30.7 ± 2.9	49.7 ± 10.8
α-[^{125}I]BTX	39.4 ± 3.7	134.2 ± 15.0	4.6 ± 3.3	7.7 ± 5.0	5.3 ± 3.5

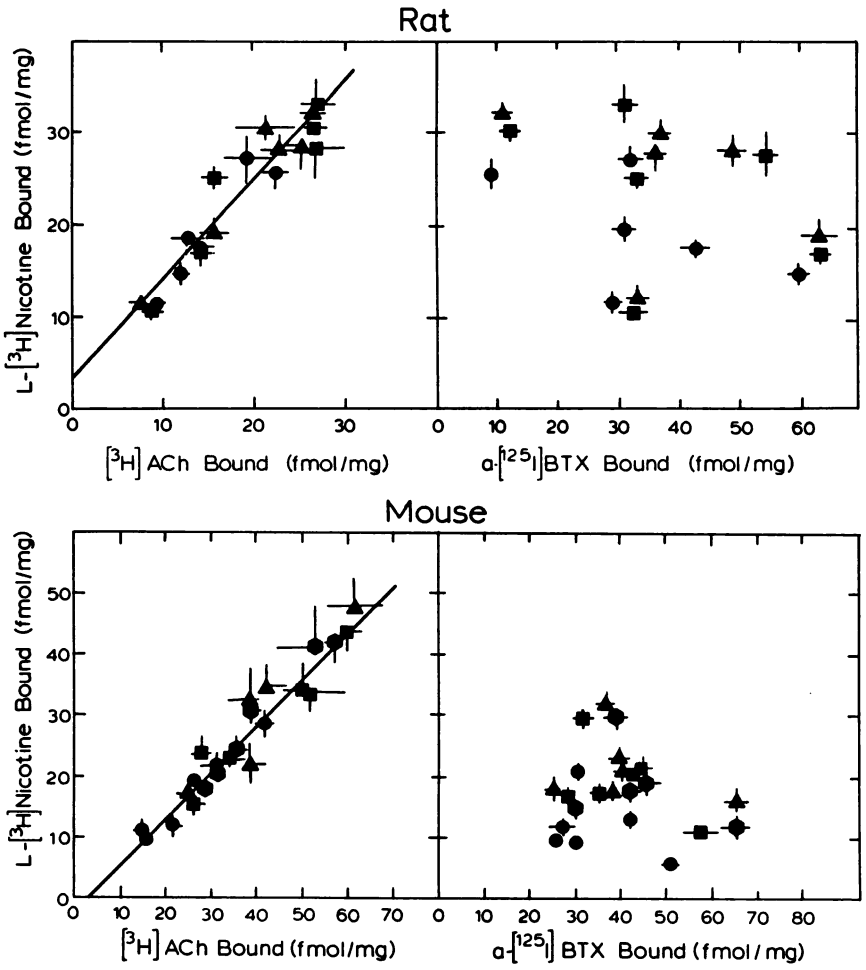

Fig. 7. Response to chronic nicotine treatment. Rats and mice were treated chronically with nicotine as described in Materials and Methods. After treatment, six brain regions were dissected and assayed for the binding of the three ligands. Treatment levels are indicated as follows: Rat, saline (●), 0.8 mg/kg twice daily (■), or 1.6 mg/kg twice daily (▲); *Mouse*, saline (●), 2.0 mg/kg/hr (■), 4.0 mg/kg/hr (▲), or 6.0 mg/kg/hr (●). Each *point* represents the mean ± standard error for six to nine individual measurements. The equations of the lines are: rats, nicotine versus ACh, $Y = 1.08X + 3.48$, $r = 0.95$; nicotine versus α-BTX, $Y = -0.16X + 28.36$, r −0.33; and mice, nicotine versus ACh, $Y = 0.78X - 2.77$, $r = 0.96$, nicotine versus α-BTX, $Y = -0.09X + 21.26$, $r = -0.18$.

to a single site of high affinity in contrast to reports suggesting that [^{3}H]nicotine binding may occur to a low affinity site as well (10–13, 26), or even exhibit positive cooperativity in its binding interactions (27). Although the reasons for these discrepancies are not clear, the low affinity binding site for nicotine may arise from proteolysis during tissue preparation (28). In our previous report (12), we described a low affinity site for nicotine binding that occurred at 4°, but not at 37° when 1 mM nonradioactive nicotine was used to establish blank values. Since 10 μM nicotine (rather than 1 mM nicotine) was used to establish blank values, the low affinity site was not observed in the present study.

The effects of DTT on the nicotinic sites reported in this paper are comparable to those obtained previously for both α-[^{125}I]BTX and [^{3}H]ACh binding sites and are consistent with the hypothesis that a disulfide bond is critical for the interaction of the ligands with their binding sites (29–31).

It is as yet unclear whether the binding sites measured with any of the ligands investigated here are truly the receptors mediating nicotine actions or nicotinic cholinergic activity. Several lines of indirect evidence suggest that these binding sites may be functional receptors, however. The binding of both [^{3}H]nicotine and [^{3}H]ACh responds to chronic treatment with direct acting nicotinic agonists (increased binding) and to treatment with anticholinesterases (decreased binding) (13, 16–20). The effect of *in vivo* nicotine administration on these sites has been confirmed in the present study. Chronic nicotine treatment also increases α-[^{125}I]BTX binding in mouse brain (17, 20). This *in vivo* regulation of these postulated nicotinic receptors suggests that they may indeed have a function. This assertion is also supported by the observation that the time course of the changes of L-[^{3}H]nicotine-binding sites with chronic nicotine treatment parallels the tolerance developed for several behavioral tests (20). The amount of α-[^{125}I]BTX binding in mouse hippocampus appears to correlate with the sensitivity of mice of different genotypes to nicotine-induced convulsions (31, 32). Although more direct demonstration that these binding sites relate to a physiological response is required, the observations cited above suggest that they may each be functional.

In summary, from the results presented in this paper, the weight of evidence strongly supports the contention that the nicotinic binding of [^{3}H]ACh and the binding of L-[^{3}H]nicotine occur at the same site and, therefore, that L-[^{3}H]nicotine binding is cholinergic. It would seem reasonable to conclude, in the absence of any evidence to the contrary, that [^{3}H]ACh and L-[^{3}H]nicotine bind to the same set of sites and can be used interchangeably to measure the high affinity binding to sites with nicotinic cholinergic properties. The results do not discount the possibility that some of the effects of nicotine *in vivo* are mediated through noncholinergic sites, but it appears unlikely that those sites are measured by high affinity nicotine binding.

Acknowledgments

The authors wish to thank Dr. Takuro Kasaki, of the Japan Tobacco and Salt Public Corporation (Yokohama, Japan), for supplying the D-(+)-nicotine. We

also wish to thank Cindy Murphy-Erdosh for technical assistance. Some of the supplies for this project were purchased with funds from a grant to J.M.W. (Air Force Office of Scientific Research Grant 85-0369).

References

1. Morley, B. J., G. E. Kemp, and P. Salvaterra. α-Bungarotoxin binding sites in the CNS. *Life Sci.* **24**:859–872 (1979).
2. Oswald, R. E., and J. A. Freeman. Alpha-bungarotoxin binding and central nervous system nicotinic acetylcholine receptors. *Neuroscience* **6**:1–14 (1981).
3. Lucas, R. J. Properties of curaremimetic neurotoxin binding sites in the rat central nervous system. *Biochemistry* **23**:1152–1160 (1984).
4. Conti-Tronconi, B. M., S. M. J. Dunn, E. A. Barnard, J. O. Dolly, F. A. Lai, N. Ray and M. A. Raftery. Brain and muscle nicotinic acetylcholine receptors are different but homologous proteins. *Proc. Natl. Acad. Sci. USA* **82**:5208–5212 (1985).
5. Chou, T. C., and C. Y. Lee. Effect of whole and fractionated cobra venom on sympathetic ganglion transmission. *Eur. J. Pharmacol.* **8**:326–330 (1969).
6. Melidi, R., and A. C. Szczepaniak. Effect of dendrosapis neurotoxins on synaptic transmission in the spinal cord of the frog. *Proc. R. Soc. Lond. B Biol. Sci.* **190**:267–274 (1974).
7. Duggan, A. W., J. G. Hall, and C. Y. Lee. Alpha-bungarotoxin, cobra neurotoxin and excitation of Renshaw cells by acetylcholine. *Brain Res.* **107**:166–170 (1976).
8. Schwartz, R. D., R. McGee, Jr., and K. J. Kellar. Nicotinic cholinergic receptors labeled by [^{3}H]acetylcholine in rat brain. *Mol. Pharmacol.* **22**:56–62 (1982).
9. Abood, L. G., D. T. Reynolds, and J. M. Bidlack. Stereospecific ^{3}H-nicotine binding to intact and solubilized rat brain membranes and evidence for its noncholinergic nature. *Life Sci.* **27**:1307–1314 (1980).
10. Romano, C., and A. Goldstein. Stereospecific nicotine receptors on rat brain membranes. *Science (Wash. D. C.)* **210**:647–650 (1980).
11. Sershen, H., M. E. A. Reith, A. Lajtha, and J. Gennaro, Jr. Noncholinergic saturable binding of (±)-[^{3}H]nicotine to mouse brain. *J. Recept. Res.* **2**:1–15 (1981).
12. Marks, M. J., and A. C. Collins. Characterization of nicotine binding in mouse brain and comparison with the binding of α-bungarotoxin and quinuclidinyl benzilate. *Mol. Pharmacol.* **22**:554–564 (1982).
13. Costa, L. G., and S. D. Murphy. [^{3}H]Nicotine binding in rat brain: alteration after chronic acetylcholinesterase inhibition. *J. Pharmacol. Exp. Ther.* **226**:392–397 (1983).
14. Abood, L. G., D. T. Reynolds, H. Booth, and J. M. Bidlack. Sites and mechanisms for nicotine's action in the brain. *Neurosci. Biobehav. Rev.* **5**:479–486 (1981).
15. Clarke, P. B. S., R. D. Schwartz, S. M. Paul, C. B. Pert, and A. Pert. Nicotinic binding in rat brain: autoradiographic comparison of [^{3}H]acetylcholine, [^{3}H]nicotine, and [^{125}I]-α-bungarotoxin. *J. Neurosci.* **5**:1307–1315 (1985).
16. Schwartz, R. D., and K. J. Keller. Nicotinic cholinergic receptor binding sites in brain: *in vivo* regulation. *Science (Wash. D. C.)* **220**:214–216 (1983).
17. Marks, M. J., J. B. Burch, and A. C. Collins. Effects of chronic nicotine infusions on tolerance development and cholinergic receptors. *J. Pharmacol. Exp. Ther.* **226**:806–816 (1983).
18. Morrow, A. L., R. Loy, and I. Creese. Alteration of nicotinic cholinergic agonist binding sites in hippocampus after fimbria transsection. *Brain Res.* **334**:309–314 (1985).
19. Schwartz, R. D., and K. J. Keller. *In vivo* regulation of [^{3}H]acetylcholine recognition sites in brain by nicotinic cholinergic drugs. *J. Neurochem.* **45**:427–433 (1985).
20. Marks, M. J., J. A. Stitzel, and A. C. Collins. A time course study of the effects of chronic nicotine infusion on drug response and brain receptors. *J. Pharmacol. Exp. Ther.* **235**:619–628 (1985).
21. Sershen, H., M. E. A. Reith, A. Hasim, and A. Lajtha. Comparison of [^{3}H]nicotine and [^{3}H]acetylcholine binding in mouse brain: a regional comparison. *Res. Commun. Chem. Pathol. Pharmacol.* **48**:345–352 (1985).
22. Abood, L. G., W. Latham, and S. Grassi. Isolation of a nicotine binding site by affinity chromatography. *Proc. Natl. Acad. Sci. USA* **80**:3536–3539 (1983).
23. Lowry, O. H., N. J. Rosebrough, A. L. Farr, and R. J. Randall. Protein measurement with the Folin phenol reagent. *J. Biol. Chem.* **193**:265–275 (1951).

23a. Cheng, Y.-C., and W. H. Prusoff. Relationship between the inhibition constant (K_i) and the concentration of inhibitor which causes 50 percent inhibition (IC_{50}) of an enzymatic reaction. *Biochem. Pharmacol.* **22**:3099–3108 (1973).

24. Martino, A. M., V. Hamui, and K. J. Keller. [^{3}H]acetylcholine and [^{3}H](−)nicotine label the same nicotinic cholinergic binding site in brain. *Soc. Neurosci. Abstr.* **11**:93 (1985).
25. Schwartz, R. D. Autoradiographic distribution of high affinity muscarinic and nicotinic cholinergic receptors labeled with [^{3}H]acetylcholine in rat brain. *Life Sci.* **38**:2111–2119 (1986).
26. Abood, L. G., S. Grassi, and M. Constanza. Binding of optically pure (−)-[^{3}H]nicotine to rat brain membranes. *FEBS Lett.* **157**:147–149 (1983).
27. Sloan, J. W., G. D. Todd, and W. R. Martin. Nature of nicotine binding in rat brain P_2 fraction. *Pharmacol. Biochem. Behav.* **20**:899–909 (1984).
28. Lipiello, P. M., and K. G. Fernandes. The binding of L-[^{3}H]nicotine to a single class of high affinity sites in rat brain membranes. *Mol. Pharmacol.* **29**:448–454 (1986).
29. Lukas, R. J., and E. L. Bennett. Chemical modification and reactivity of sulfhydryls and disulfides of rat brain nicotinic-like acetylcholine receptors. *J. Biol. Chem.* **225**:5573–5577 (1980).
30. Schwartz, R. D., and K. J. Kellar. [^{3}H]Acetylcholine binding sites in brain: effect of disulfide bond modification. *Mol. Pharmacol.* **24**:387–391 (1983).
31. Miner, L. L., M. J. Marks, and A. C. Collins. Relationship between nicotine-induced seizures and hippocampal nicotinic receptors. *Life Sci.* **37**:75–83 (1985).
32. Miner, L. L., M. J. Marks, and A. C. Collins. Classical genetic analysis of nicotine-induced seizures and nicotinic receptors. *J. Pharmacol. Exp. Ther.* **231**:545–554 (1984).

Send reprint requests to: Dr. Michael J. Marks, Institute for Behavioral Genetics, Campus Box 447, University of Colorado, Boulder, CO 80309.